Analytical Methods

Accepted Manuscript

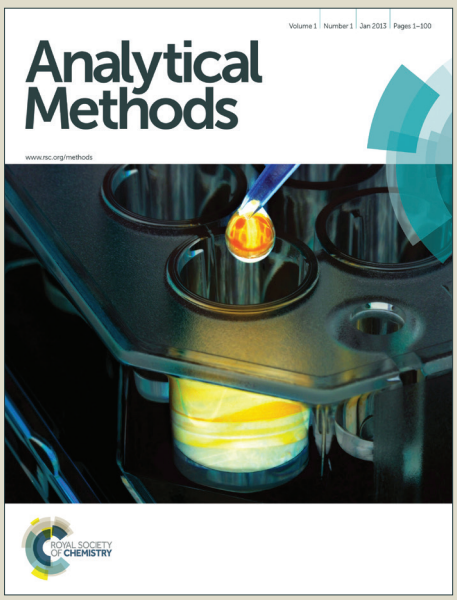

ROYAL SOCIETY OF CHEMISTRY

www.rsc.org/methods

Cite this: DOI: 10.1039/c0xx00000x

www.rsc.org/xxxxxx

ARTICLE TYPE

Fluorescent Ratiometric Cu^{2+} Probe Based on FRET by Naphthalimide-Appended Rhodamine Derivative

Chunwei Yu,[a] Yingying Wen,[a] Xi Qin*[,b] and Jun Zhang*[,a]

Received (in XXX, XXX) Xth XXXXXXXXX 20XX, Accepted Xth XXXXXXXXX 20XX

DOI: 10.1039/b000000x

A fluorophore dyad (**L**) containing rhodamine B and naphthalimide units linked through C=N was constructed as a ratiometric probe for Cu^{2+}. The selective fluorescent response of the probe **L** to Cu^{2+} was triggered by Cu^{2+} induced ring-opening process of the rhodamine B spirolactam, which was based on an intramolecular fluorescence resonance energy transfer (FRET) mechanism from naphthalimide to rhodamine B. The system exhibited high selectivity for Cu^{2+} as compared to other tested metal ions and anions, and signaled the binding event through occurrence of FRET mediated emission at 580 nm of the rhodamine chromophore with enhancement in the fluorescence intensity, concurrently, the featured emission of the naphthalimide donor at around 525 nm was nearly completely quenched. Furthermore, it has been used for ratiometric imaging of Cu^{2+} in living cells with satisfying results.

Introduction

The selective binding of chemical species upon molecular recognition can lead to large perturbations in the host environment, particularly when the guest is ionic. Thus, the design and development of small molecules for sensing applications are of great interest. Fluorescent probes are powerful tools for monitoring biologically relevant species *in vitro* detection and/or *in vivo* bioimaging by virtue of their simplicity and high sensitivity.[1] Especially the widespread use of confocal light microscopy has inspired chemists to develop functional fluorescent reagents that respond to intracellular events, thus offering a powerful set of chemical probes for studying fundamental aspects of cell physiology. Accordingly, lots of probes used for the detection of different targets have been successfully designed,[2] these reported fluorescent probes widely use signaling mechanisms of photo-induced electron transfer (PET),[2] intramolecular charge transfer (ICT),[3] excimer/exciplex formation,[4] and fluorescence resonance energy transfer (FRET),[5-8] etc. Among them, FRET is unique in generating fluorescence signals sensitive to molecular conformation, association and separation in the 1–10 nm range.[5] More importantly, FRET imaging that affords simultaneous recording of two emission intensities at different wavelengths in the presence and absence of analytes has provided a facile method for visualizing complex biological processes at the molecular level.[9] However, most of reported FRET imaging is focused on recognizing biomacromolecules, and only few FRET-based probes have been used to monitor low-weight molecular species (especially metal ions) in living samples although some metal ions play important roles in biological systems.[5,6,10,11]

Cu^{2+} is an essential element in living systems and has an extremely ecotoxicological impact on the human health.[12] However, Cu^{2+} exhibits toxicity under overloading conditions in that it causes neurodegenerative diseases.[13] Thus, it is necessary to trace the concentration of Cu^{2+} *in vitro* and *in vivo*, and many studies focus on the design of fluorescent probes and the analysis of Cu^{2+} have been reported.[14] Because FRET is a nonradiative energy transfer process in which the excitation energy of the donor is transferred to the nearby acceptor via long-range dipole-dipole interaction and/or short-range multipolar interaction, it is mainly determined by the extent of the spectral overlap between the donor emission and acceptor absorption.[7] Therefore, it would be possible to fabricate a ratiometric probe based on the FRET mechanism if a molecule could generate a suitable fluorescent energy acceptor by the interaction with target analyte. It is pitiful that only a few studies have been reported based on FRET for the detection of Cu^{2+}.[15]

As we all know, rhodamine derivatives have excellent photophysical properties, and many fluorescent probes derived from rhodamine have been successfully used as for the detection of metal ion, anions, et al.[16] The naphthalimide derivatives have broad fluorescence emission spectrum (450-650 nm), which covered a part of absorption of rhodamine (500-560 nm) and fulfilled a favorable condition for FRET. Kept this in mind, a fluorescent probe comprised of a naphthalimide donor and a rhodamine acceptor was designed for ratiometric detection of Cu^{2+} based on FRET, and this new probe **L** was successfully used for FRET imaging Cu^{2+} in living cells.

Experimental

Apparatus

NMR spectra were collected in DMSO-d_6 at 25 °C on a Bruker WM–300 spectrometer. Electrospray ionization (ESI) analyses were performed on a Thermo TSQ Quantum Mass Spectrometer.

UV-Vis spectra were obtained on a Beckman DU–800 spectrophotometer with 1 cm quartz cell at 25 °C. Fluorescence measurements were carried out on a HORIBA Fluoromax-4 luminescence spectrometer. Fluorescence imaging was performed by confocal fluorescence microscopy on an Olympus FluoView Fv1000 laser scanning microscope. pH values were measured with a pH-meter PBS-3C.

Materials

All reagents and solvents are of analytical grade and used without further purification. Metal ions species employed were from NaCl, $MgCl_2·6H_2O$, $CdCl_2$, $HgCl_2$, $CaCl_2·2H_2O$, $FeCl_3·6H_2O$, $CrCl_3·6H_2O$, $Zn(NO_3)_2·6H_2O$, $AgNO_3$, $CoCl_2·6H_2O$, $MnCl_2·4H_2O$, $CuCl_2·2H_2O$, $NiCl_2·6H_2O$, and $PbCl_2$, respectively. Anion species from various salts such as NaClO, $NaNO_3$, Na_2CO_3, NaCl, NaAc, KBr, Na_2S, NaSCN and Na_2HPO_4. Metal ions and anions were dissolved in deionized water and probe was dissolved in DMSO to obtain 1.0 mM stock solutions, respectively.

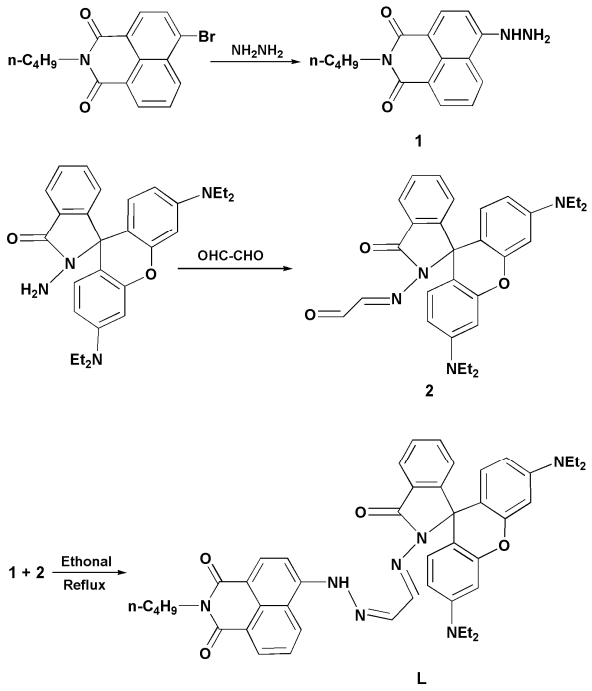

Scheme 1. Chemical structure and synthesis route of probe **L**.

Synthesis

The synthesis route of probe **L** was shown in **Scheme 1**.

The synthesis of probe **L**. 1.0 mmol compound **1**[17] (0.283 g) and 1.0 mmol compound **2**[14b-e] (0.496 g) were mixed in 50 mL absolute ethanol and refluxed for 4 h. After the reaction was finished, the precipitate so obtained was filtered and purified with silica gel column chromatography (CH_2Cl_2/acetic ether = 7:1, v/v) to afford **L** as red-brown solid. Yields: 87.2 %. MS: m/z 762.34 $[M + H]^+$. ^1H NMR (d_6-DMSO, δ ppm): 11.46 (s, 1H), 8.64 (d, 1H, J = 8.55), 8.59 (d, 1H, J = 8.25), 8.47 (d, 1H, J = 7.25), 8.34 (d, 1H, J = 8.45), 7.92 (d, 2H, J = 8.40), 7.78 (t, 1H, J = 7.90), 7.63 (t, 1H, J = 7.37), 7.57 (t, 1H, J = 7.40), 7.49 (d, 1H, J = 8.45), 7.09 (d, 1H, J = 7.60), 6.46 (d, 2H, J = 7.70), 6.43 (s, 2H), 6.36 (d, 2H, J = 8.95), 4.01 (t, 2H, J = 7.35), 3.32 (m, 8H, J = 6.93), 1.59 (m, 2H, J = 7.42), 1.33 (m, 2H, J = 7.38), 1.09 (t, 12H, J = 6.97), 0.91 (t, 3H, J = 7.37). ^{13}C NMR (d_6-DMSO, δ ppm): 164.55, 164.01, 163.38 (C=O), 162.77, 152.96, 151.96, 149.04 (ArC), 145.96, 145.57 (C=N), 143.67, 134.72, 133.63, 132.17, 131.99, 131.38, 129.40, 129.35, 129.13, 128.55, 128.43, 128.06, 125.86, 124.28, 123.64, 122.58, 119.32, 112.78, 108.60, 107.93, 105.46, 97.83 (ArC), 65.98, 44.14, 36.25, 30.21, 20.28, 14.20, 12.88.

UV-Vis and fluorescence titration

Test solutions were prepared by placing 100 μL of the **L** stock solution (1 mM) into a test tube, adding an appropriate aliquot of individual ions stock solution (1 mM), and then diluting the solution to 5 mL with ethanol/water (1:9, v/v, 50 mM HEPES, pH 7.4). For pH effect study, a series of HEPES buffers (50 mM) were prepared with different pH values adjusted by adding certain amounts of 1.0 M HCl or 1.0 M NaOH. All of the UV-Vis and fluorescence titration data were recorded at room temperature. For all fluorescence measurements, excitation and emission slit widths were 3 nm and 3 nm, respectively.

Cell incubation and imaging

RAW cells placed on coverslips were washed with phosphate-buffered saline (PBS), followed by incubating with 10 μM of $CuCl_2$ (in PBS) for 30 min at 37 °C, and then washed with PBS three times. After incubating with 20 μM of probe L for 30 min at 37 °C, and then the cells were washed with PBS three times again. Fluorescence imaging of intracellular Cu^{2+} in RAW cells was conducted by using a confocal fluorescence microscopy on an Olympus FluoView Fv1000 laser scanning microscope.

Results and discussion

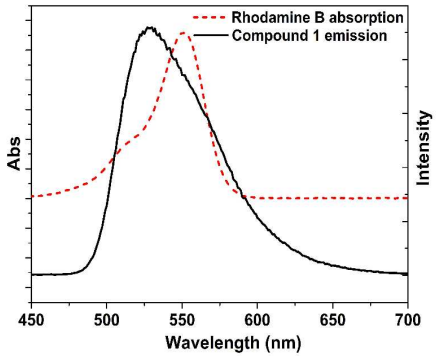

Fig. 1. Spectral overlap of the donor **1** emission with the acceptor rhodamine B absorption.

Absorption and fluorescence spectra of rhodamine B and compound 1.

The absorption and the emission spectra of rhodamine B and compound **1** (including donor and acceptor) of **L** were shown in **Fig. 1**. Notably, naphthalimide exhibits emission at 525 nm when excited at 355 nm, the maximum absorption peak at 556 nm of rhodamine B at the ring-opened form overlaps with the emission spectrum of naphthalimide, fulfilling a favorable condition for FRET. In the new developed sensing system, the emission peaks between naphthalimide and rhodamine B were well-resolved,

which can avoid the emission spectra overlap problem generally met by spectra-shift type probes. Futhermore, fluorescence signal change at two different emission wavelengths with high resolution also benefited for a large range of emission ratios, thereby a high sensitivity for Cu^{2+} detection was conducted.

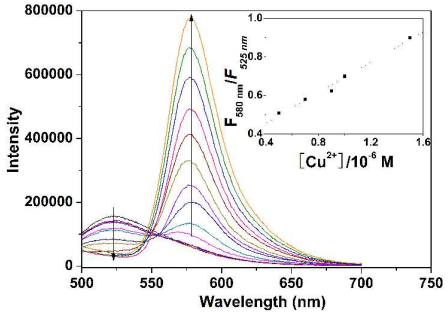

Fig. 2. Fluorescence titration spectra of **L** (2 μM) in ethanol/water solution (1:9, v/v, 50 mM HEPES, pH 7.4) upon gradual addition of Cu^{2+} (0-10 μM). Inset: Fluorescence intensity ratio changes ($F_{580\ nm}/I_{525\ nm}$) of **L** upon gradual addition of Cu^{2+}. Ex = 355 nm.

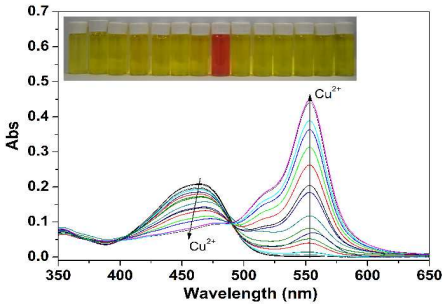

Fig. 3. Changes in absorption spectra of **L** (5 μM) in ethanol/water solution (1:9, v/v, 50 mM HEPES, pH 7.4) with various amounts of Cu^{2+} (0-50 μM). Inset: photograph of **L** (20 μM) as a selective naked-eye probe for Cu^{2+} upon addition of 100 μM individual metal ion including blank, Ag^{+}, Ca^{2+}, Mg^{2+}, Zn^{2+}, Pb^{2+}, Cu^{2+}, Hg^{2+}, Cd^{2+}, Co^{2+}, Ni^{2+}, Mn^{2+}, Cr^{3+} and Fe^{3+} (from left to right).

Fluorescent and colorimetric signaling of Cu^{2+}

The fluorescence spectrum of compound **L**, in the absence of Cu^{2+}, exhibited emission at 525 nm attributed to 1, 8-naphthalimide donor by excitation of 355 nm. The rhodamine B moiety adopted a closed, non-fluorescent spirolactam form, spectral overlap between 1, 8-naphthalimide emission and rhodamine absorption is minimized, and as a result, FRET is suppressed. Upon selective binding to Cu^{2+} (0-10 μM) in the solution of **L**, a new emission band characteristic of the acceptor component appeared at 580 nm corresponded to the opening of the spirolactam ring of rhodamine B to an amide form (the energy acceptor). Meanwhile, the donor emission at 525 nm decreased. Spectral overlap was enhanced, the subsequent FRET process of **L** are triggered by Cu^{2+}, the linear fluorescence enhancement of **L** (2 μM) toward amounts of Cu^{2+} added was obtained in the range of 0.5–1.5 μM (R = 0.999) (Inset of **Fig. 2**). The limit of detection (LOD) was attained of 0.25 μM, based on $3 \times \delta_{blank}/k$ (where δ_{blank} is the standard deviation of the blank solution and k is the slope of the calibration plot). The transformation of **L** was also supported by fluorescent emission at 580 nm excited by 520 nm light (**Fig. S1**, in the supporting information). The absorption properties of **L** in ethanol/water solution (1:9, v/v, 50 mM HEPES, pH 7.4) were also determined. **L** showed only the absorption profile of the donor (naphthalimide), which had a maximum at 463 nm. Notably, upon sequential addition of Cu^{2+} to the **L** solution induced an increase in the absorption intensity at 556 nm, which corresponded to the absorption of rhodamine B (**Fig. 3**), corresponding to a change in color from weak yellow to pink as shown in the inset of **Fig. 3**. Meanwhile, the band at 463 nm decreased gradually in intensity, with an isosbestic point at 490 nm. These facts indicated that **L** was induced to form the open-ring structure from the spirolactam form by Cu^{2+}.

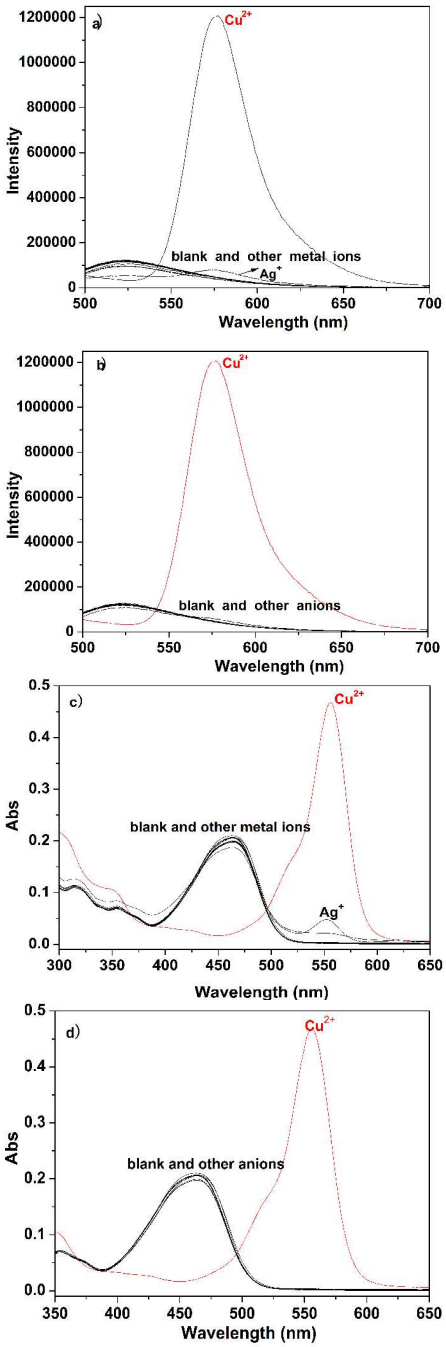

Fig. 4. The fluorescence (a, b) and absorption (c, d) spectra of **L** (2 μM and 5 μM, respectively) in ethanol/water solution (1:9, v/v. 50 mM HEPES, pH 7.4) upon addition of 50 μM Cu^{2+} and other metal ions and anions, including of Na^{+}, Ag^{+}, Zn^{2+}, Pb^{2+}, Co^{2+}, Cd^{2+}, Ni^{2+}, Ca^{2+}, Mg^{2+}, Hg^{2+}, Cr^{3+}, Fe^{3+}, ClO^{-}, NO_3^{-}, CO_3^{2-}, Ac^{-}, Br^{-}, Cl^{-}, SO_4^{2-}, SCN^{-}, HPO_4^{2-} and S^{2-}.

Interference studies from other metal ions and anions

To further investigate the selectivity of probe **L**, fluorescence and UV-Vis responses of **L** toward various metal ions and anions were carried out. In the mixed aqueous media, most of metal ions (Na^+, Ag^+, Zn^{2+}, Pb^{2+}, Co^{2+}, Cd^{2+}, Ni^{2+}, Ca^{2+}, Mg^{2+}, Hg^{2+}, Cr^{3+} and Fe^{3+}) and anions (ClO^-, NO_3^-, CO_3^{2-}, Cl^-, Ac^-, Br^-, SO_4^{2-}, SCN^-, HPO_4^{2-} and S^{2-}), except for Ag^+, which promoted a slight effect, did not lead to any significant fluorescence and absorption changes in the visible region (**Fig. 4**). In addition, to check the practical ability of **L** as a Cu^{2+} selective fluorescent probe, we carried out competitive experiments in the presence of Cu^{2+} mixed with 10 equiv. other metal ions and anions. As shown in **Fig. S2** in the supporting information, the ratiometric fluorescence changes resulting from the addition of Cu^{2+} was not influenced by the subsequent addition of the other metal ions and anions.

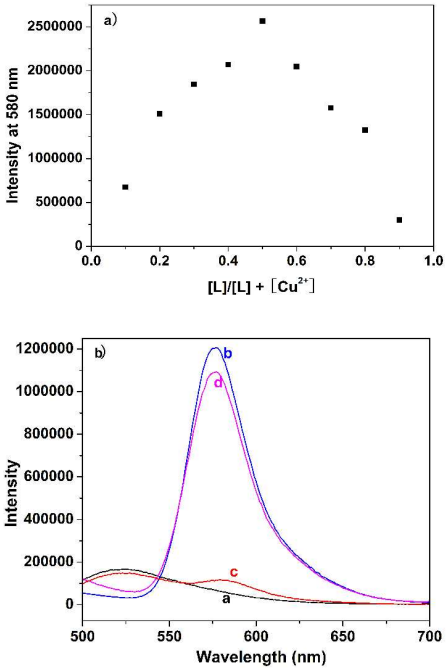

Fig. 5. (a) Job's plot for determining the stoichiometry of **L** and Cu^{2+}. The total concentration was kept 20 μM; **(b)** Fluorescence spectra of the reversibility behavior of **L** with Cu^{2+}. a: blank (2 μM); b: blank (2 μM) + Cu^{2+} (50 μM); c: blank (2 μM) + Cu^{2+} (50 μM) + EDTA (200 μM); d: blank (2 μM) + Cu^{2+} (50 μM) + EDTA (200 μM) + Cu^{2+} (200 μM).

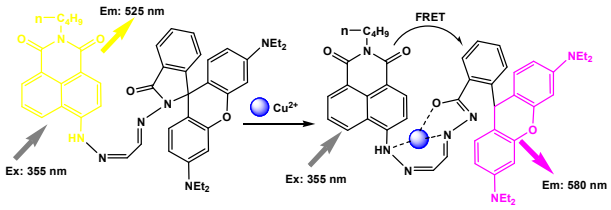

Scheme 2. Binding mode of **L** with Cu^{2+}.

Possible sensing mechanism

The method of continous variation (Job's plot) clearly confirmed the 1:1 stoichiometry **L** with Cu^{2+}, as shown in **Fig. 5(a)**, which was also supported by ESI-MS (**Fig. S3**, in the supporting information), where main peak at 869.14 corresponded to $[\mathbf{L} + Cu^{2+} + CH_3CH_2OH - H^+]^+$. We also carried out a reversibility experiment, as shown in **Fig. 5(b)**. In the presence of EDTA, because of the stronger affinity between EDTA-Cu^{2+}, it resulted in the decomplexation of **L**-Cu^{2+} complex. On further addition of Cu^{2+}, the fluorescence intensity was revived again indicating the reversible behavior of **L** for Cu^{2+}. The proposed binding mode of **L** with Cu^{2+} was illustrated in **Scheme 2**.

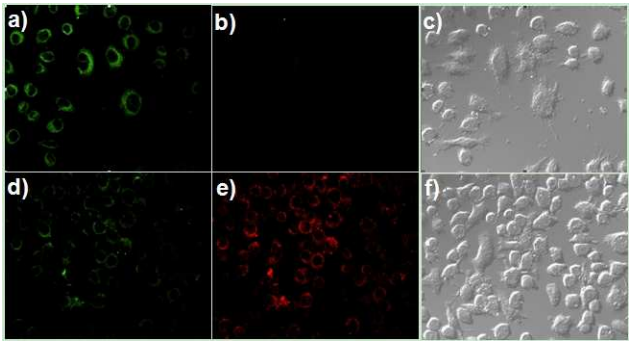

Fig. 6. FRET images in RAW cells. (Top, a–c) Cells incubated with 20 μM **L** for 30 min. (Bottom, d–f) Cells incubated with both 10 μM Cu^{2+} and 20 μM **L** for 30 min. Emission was collected by the green channel at 520 ± 20 nm (a and d) and the red channel at 600 ± 40 nm (b and e). (c and f) Bright field imaging. ex = 404 nm

Fluorescence imaging of living cells for Cu^{2+}

The hydrophilicity of the rhodamine moiety and the lipophilicity of the naphthalimide moiety mean that probe **L** has the advantage of proper amphipathicity and can be dissolved in mixtures of organic solvents and water. It is a very important factor for both cell permeability and intracellular fluorescent imaging. We proceeded to evaluate the potential biological applications of **L** in vitro detection of Cu^{2+} in RAW cells. The double-channel fluorescence images at (520 ± 20) and (600 ± 40) nm are shown in Fig. 6 as **L** was excited at 404 nm. RAW cells incubated with **L** (20 μM) for 30 minutes at 37 °C led to a clear green intracellular fluorescence, which suggested that **L** was cell permeable (**Fig. 6a**). However, cells supplemented with $CuCl_2$ (10 μM) were then treated with **L** (20 μM) under same conditions, a remarkable increase in the red fluorescence intensity (**Fig. 6e**) and a partial quenching of the green fluorescence intensity (**Fig. 6d**) was observed. Meanwhile, brightfield measurements after treatment with Cu^{2+} and **L** revealed that the cells remained viable and no apparent toxicity were observed throughout the imaging experiments.

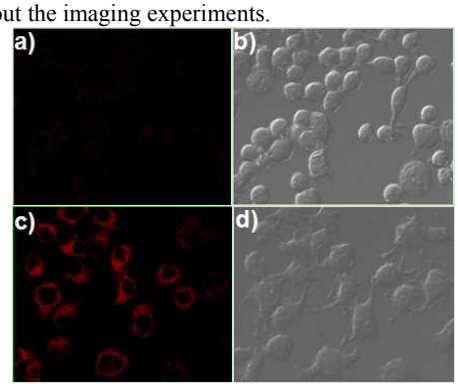

Fig. 7. Confocal fluorescence images in RAW cells. a) Cells incubated with 20 μM **L** in PBS buffer for 30 min; b) Brightfield image of cells shown in panel a); c) Cells incubated with 10 μM Cu^{2+} for 30 min, washed three times, and then further incubated with 20 μM **L** for 30 min; d) Brightfield image of cells shown in panel c). ex = 559 nm

Furthermore, under selectively excitation of the rhodamine moiety of **L** with longer-wavelength light at 559 nm, staining RAW cells with a 20 μM solution of **L** for 30 min at 37 ^{o}C gave very weak intracellular fluorescence (**Fig. 7a**). Upon addition of 10 μM $CuCl_2$ to **L**-loaded RAW cells in the growth medium for 30 min at 37 ^{o}C, a significant increase in the fluorescence from the intracellular area was observed (**Fig. 7c**). These experiments indicate that **L** can provide ratiometric detection for intracellular Cu^{2+}. Therefore, it could be a useful molecular probe for studying biological processes involving Cu^{2+} within living cells.

Method performance comparison

The photophysical properties of typical FRET based Cu^{2+} probes were summarized (**Table S1**).[15] Though the availability of fluorescence is increasing, there are still numerous challenges and opportunities remaining for development of new fluorophores and practical applications in biological systems, such as signal output,[15a] testing media[15a] and applicability.[15a-d] Our newly developed probe based on FRET presents a number of attractive analytical features such as testing media and wide applicability. It can be used for rapid analysis of ultra-trace level Cu^{2+} in living cells with satisfactory results.

Conclusions

In summary, we have presented the synthesis and properties of **L**, a new FRET-based ratiometric Cu^{2+} probe. It exhibits a clear Cu^{2+}-induced change in the intensity ratio of the two emission bands of naphthalimide and rhodamine. Moreover, confocal fluorescence microscopy confirmed that **L** can be used for monitoring intracellular Cu^{2+} levels in living cells with general fluorescence and FRET methods. Thus, we expect the strategy will serve as practical tool for environmental samples analysis and biological studies.

Acknowledgements

This work was financially supported by the National Natural Science Foundation of China (No. 81260268, 81360266), the Natural Science Foundation of Hainan Province (No. 812188, 413131), the Colleges and Universities Scientific Research Projects of the Education Department of Hainan Province (Hjkj2013-29).

Notes and references

[a] *Laboratory of Environmental Monitoring, School of Tropical and Laboratory Medicine, Hainan Medical University, Haikou, 571101, China. Fax: +86 898 66989173; Tel: +86 898 66973190; E-mail: jun_zh1979@163.com*

[b] *Department of Clinical Laboratory, Affiliated Hospital of Hainan Medical University, Haikou 570102, China. Fax: +86 898 66989173; Tel: +86 898 66773727; E-mail: qinxi99@21cn.com*

† Electronic Supplementary Information (ESI) available: [details of any supplementary information available should be included here]. See DOI: 10.1039/b000000x/

1 (a) R. W. Duke, E. B. Veale, F. M. Pfeffer, P. E. Kruger and T. Gunnlaugsson, *Chem. Soc. Rev.*, 2010, **39**, 3936; (b) S. Liu, S. Pang, W. Na and X. Su, *Biosens. Bioelectron.*, 2014, **55**, 249; (c) X. H. Gao, X. H. Li, Q. Q. Wan, Z. Li and H. M. Ma, *Talanta*, 2014, **120**, 451.

2 (a) G. Sivaraman, T. Anand and D. Chellappa, *RSC Adv.*, 2012, **2**, 10605; (b) S. K. Kim, S. H. Lee, J. Y. Lee, J. Y. Lee, R. A. Bartsch and J. S. Kim, *J. Am. Chem. Soc.*, 2004, **126**, 16499.

3 H. H. Wang, L. Xue, Y. Y. Qian and H. Jiang, *Org. Lett.*, 2010, **12**, 292.

4 L. Liu, D. Q. Zhang, G. X. Zhang, J. F. Xiang and D. B. Zhu, *Org. Lett.*, 2008, **10**, 2271.

5 Z. G. Zhou, M. X. Yu, H. Yang, K. W. Huang, F. Y. Li, T. Yi and C. H. Huang, *Chem. Commun.*, 2008, **29**, 3387.

6 M. Kumar, N. Kumar, V. Bhalla, H. Singh, P. R. Sharma and T. Kaur, *Org. Lett.*, 2011, **13**, 1422.

7 Y. L. Liu, X. Lv, Y. Zhao, M. L. Chen, J. Liu, P. Wang and W. Guo, *Dyes Pigm.*, 2012, **92**, 909.

8 M. Kumar, N. Kumar, V. Bhalla, H. Singh, P. R. Sharma and T. Kaur, *Org. Lett.*, 2011, **13**, 1422.

9 X. Wang, L. Cui, N. N. Zhou, W. P. Zhu, R. Wang, X. H. Qian and Y. F. Xu, *Chem. Sci.*, 2013, **4**, 2936.

10 M. Mank, D. F. Reif, N. Heim, M. W. Friedrich, A. Borst and O. Griesbeck, *Biophys. J.*, 2006, **90**, 1790.

11 M. J. Ruedas-Rama, X.J. Wang and E. A. H. Hall, *Chem. Commun.*, 2007, **15**, 1544.

12 R. A. Lovstad, *BioMetals*, 2004, **17**, 111.

13 N. Shao, Y. Zhang, S. M. Cheung, R. H. Yang, W. H. Chan, T. Mo, K. A. Li and F. Liu, *Anal. Chem.*, 2005, **77**, 7294.

14 (a) G. Sivaraman, T. Anand and D. Chellappa, *RSC Adv.*, 2013, **3**, 17029; (b) C. W. Yu, J. Zhang, R. Wang and L. X. Chen, *Org. Biomol. Chem.*, 2010, **8**, 5277; (c) J. Zhang, C. W. Yu, S. Y. Qian, G. Lu and J. L. Chen, *Dyes Pigm.*, 2012, **92**, 1370; (d) C. W. Yu, J. Zhang, J. H. Li, P. Liu, P. H. Wei and L. X. Chen, *Microchim Acta*, 2011, **174**, 247; (e) C. W. Yu, L. X. Chen, J. Zhang, J. H. Li, P. Liu, W. H. Wang and B. Yan, *Talanta*, 2011, **85**, 1627.

15 (a) H. J. Kim, S. Y. Park, S. Yoon and J. S. Kim, *Tetrahedron*, 2008, **64**, 1294; (b) S. Y. Lee, H. J. Kim, J. S. Wu, K. No and J. S. Lim, *Tetrahedron Lett.*, 2008, **49**, 6141; (c) V. S. Jisha, A. J. Thomas, and D. J. Ramaiah, *Org. Chem.*, 2009, **74**, 6667; (d) L. Yuan, W. Y. Lin, B. Chen and Y. N. Xie, *Org. Lett.*, 2012, **14**, 432; (e) Y. C. Chen, C. C. Zhu, J. J. Cen, J. Li, W. J. He, Y. Jiao and Z. J. Guo, *Chem. Commun.,* 2013, **49**, 7632; (f) C. Kar, M. D. Adhikari, A. Ramesh and G. Das, *Inorg. Chem.*, 2013, **52**, 743; (g) X. Y. Guan, W. Y. Lin and W. M. Huang, *Org. Biomol. Chem.*, 2014, **12**, 3944; (h) Z. J. Hu, J. W. Hu, Y. Cui, G. N. Wang, X. J. Zhang, K. Uvdalb and H. W. Gao, *J. Mater. Chem. B*, 2014, **2**, 4467.

16 (a) G. Sivaraman, T. Anand and D. Chellappa, *Analyst*, 2012, **137**, 5881; (b) G. Sivaraman and D. Chellappa, *J. Mater. Chem. B*, 2013, **1**, 5768; (c) G. Sivaraman, V. Sathiyaraja and D. Chellappa, *J. Lumin.*, 2014, **145**, 480; (d) G. Sivaraman, B. Vidya and D. Chellappa, *RSC Adv.*, 2014, **4**, 30828; (e) X. Q. Chen, T. Pradhan, F. Wang, J. S. Kim and J. Yoon, *Chem. Rev.*, 2012, **112**, 1910; (f) Y. Zhou, J. Yoon, *Chem. Soc. Rev.*, 2012, **41**, 52; (g) H. N. Kim, M. H. Lee, H. J. Kim, J. S. Kim and J. Yoon, *Chem. Soc. Rev.*, 2008, **37**, 1465.

17 J. Gan, H. Tian, Z. H. Wang, K. Chen, J. Hill, P. A. Lane, M. D. Rahn, A. M. Fox and D. D. C Bradley, *J. Organomet. Chem.*, 2002, **645**, 168.